Journal of Nuclear Materials 382 (2008) 103–111

Contents lists available at ScienceDirect

Journal of Nuclear Materials

journal homepage: www.elsevier.com/locate/jnucmat

Relevancy of displacement cascades features to the long term point defect cluster growth

M. Hou [a,*], A. Souidi [b], C.S. Becquart [c], C. Domain [d], L. Malerba [e]

[a] Physique des Solides Irradiés et des Nanostructures CP234, Université Libre de Bruxelles, Bd du Triomphe, B-1050 Bruxelles, Belgium
[b] Centre Universitaire Dr. Moulay Tahar de Saida, BP138 En Nasr, Saida 20000, Algeria
[c] Laboratoire de Métallurgie Physique et Génie des Matériaux, UMR 8517, Université Lille-1, F-59655 Villeneuve d'Ascq Cédex, France
[d] EDF-R&D Département MMC, Les renardières, F-77818 Moret sur Loing Cédex, France
[e] SCKCEN, Reactor Materials Research Unit, B-2400 Mol, Belgium

ARTICLE INFO

PACS:
61.80.Az
61.82.Bg
61.80.Hg

ABSTRACT

Displacement cascades in iron have been generated by means of the MARLOWE binary collision approximation (BCA) code with primary knock-on atom (PKA) energies ranging from 5 to 100 keV. They serve as input for modelling long term evolution by means of the LAKIMOCA Object Kinetic Monte Carlo code. It is found that the size distributions of the fractions of vacancy and interstitial clustered in the long term are not significantly dependent on the PKA energy in this range. Since the subcascade formation, morphology and spatial extension, as well as the spatial correlations between primary point defect positions do depend on the PKA energy, it is concluded that the size distributions of clustered point defects fractions in the long term do not depend on these cascade features. In contrast, the size distributions of clustered point defect fractions in displacement cascades are found to be independent of the PKA energy while their spatial correlations strongly influence the cluster size distributions in the long term. The use of a mean field approximation in cluster growth kinetics predictions is thereby invalidated. Irradiation dose and dose-rate are also found to be determinant factors governing the long term evolution.

1. Introduction

Neutrons or ions impinging on a material are well-known to produce damage in it by knocking on atoms (primary knock-on atoms, or PKAs) which then lose the acquired energy, to a large extent by displacing other atoms, in a sequence known as a displacement cascade. The cascade development is characterised by an initial ballistic phase, a subsequent thermal spike and finally a relaxation stage. The overall process lasts in the picoseconds range. Cascade processes can be simulated at the atomic level by means of molecular dynamics (MD) [1] or its binary collision approximation (BCA) [2]. At the end of the cascade, a debris is left, formed by point defects and clusters thereof, concentrated in a volume of only a few hundreds nm^3 [3,4] and distributed in a way that reflects the complex mechanisms whereby they were produced. This is the so-called primary damage. The rearrangement of these defects by diffusion and mutual reactions over tens of years of continuous irradiation produces microstructural changes that directly affect the mechanical properties and even the integrity of the material. The problem of modelling all of these processes in a predictive way is thus of primary importance for the safety of existing nuclear power plants and a large effort in this direction, based on a multiscale approach, is being made [5]. In this framework, very different time- and length-scales need to be bridged, by reducing at each step the number of variables involved. For example, atomic scale systems are characterised by a number of degrees of freedom of the order of the Avogadro number (10^{23}), but can be described according to statistical mechanics by only a few macroscopic variables, namely temperature, pressure and concentration (when different chemical species are present). In the present case, the problem addressed is the following: in a displacement cascade regime, the primary damage state is defined by the point defect spatial distributions produced after each cascade. These distributions can be statistically analysed starting from the coordinates of the defects and characterised by functions describing the spatial correlations between vacancies and self-interstitial atoms (SIAs), such as pair correlation functions, cascade volumes, elongations, etc. The primary damage has been thereby shown to be different from a purely random point defect distribution [4,6], consistently with the fact that it is the consequence of physical processes governed by given interatomic interactions and by the crystal lattice. The evolution of the initial defect distributions, according to the migration properties of point defects and their clusters and to the possible mutual reactions, leads eventually to the

* Corresponding author. Tel.: +32 2 650 5735; fax: +32 2 650 5227.
E-mail address: mhou@ulb.ac.be (M. Hou).

0022-3115/$ - see front matter © 2008 Elsevier B.V. All rights reserved.
doi:10.1016/j.jnucmat.2008.08.034

formation of a microstructure, characterised by another distribution of point defects, describable in terms of a cluster size distribution. This final distribution is regarded here as the transformation of the initial one via a 'transfer function', determined by the defect diffusion properties and mutual reactions included in the model. The objective is to identify the reduced number of parameters, defining the primary damage state produced by a cascade, that mainly determine the cluster formation and growth in the long term. An extensive comparison between different primary damage databases and the different microstructure evolutions corresponding to each of them, modelled by applying an object kinetic Monte Carlo (OKMC) method [7], revealed that dramatic differences in the initial primary damage state, particularly in terms of defect clustered fractions, are largely smoothed away in the final microstructure [8–10]. The features of the 'transfer function' appear therefore to be more important in determining the final state than the initial distributions themselves. Nonetheless, if totally random initial point defect distributions are used as input, the final microstructure is found to be significantly different [8], thereby suggesting that some of the features of the defect distributions after a cascade must be of relevance in determining the microstructure evolution [10]. Here we present an attempt at distinguishing some of these features from others. Note that the scope of this work is limited to exploring the effect of the spatial inhomogeneities intrinsic to cascade damage production on the microstructure evolution. A detailed account of possible spectral effects, related to specifics modes of irradiation (electrons, protons, neutrons of different origin, ions, ...) is beyond the scope of the present work.

Section II provides a brief summary of the simulation models and of the distributions employed to characterise the primary damage state. The relationship between cascade debris features and size distributions of clustered point defects in the long term is described and discussed in Section III. Section IV considers the variations introduced in the results by dose and dose-rate changes. A discussion is given in Section V and the main conclusions are drawn in Section IV.

2. The models

In this work a set of displacement cascade debris in iron produced using the BCA was employed for the study of the corresponding microstructural evolution. BCA cascades and their evolution on the long term have been compared with the same features assessed from a fairly large existing MD cascade database [5,11]. Also in the present work, when necessary MD cascades produced by Stoller et al. [10,11] using the code Moldy [12] and the Finnis–Sinclair many-body potential for iron [13], were used. The primary damage has been characterized by treating separately the SIA and vacancy populations, using component analysis [14] coupled to a fuzzy partition technique [15] for the identification of subcascades. The latter method allows overlapping subcascades to be recognised, by finding the partition of each displacement cascade debris configuration which minimizes the overlap, without assuming a priori any subcascade prototype or number (for technical reasons, though, the algorithm cannot partition one cascade into more than 16 subcascades). Component analysis allows an ellipsoid to be associated with each subcascade and therefore to compute the corresponding volume and an aspect ratio. The latter is defined as $\alpha/\gamma-1$, where α and γ are, respectively, the major and the minor components of the correlation matrix between point defect positions, i.e. the longest and shortest semiaxes of the associated ellipsoid; it thus measures the offset from sphericity. The reader is referred to Refs. [4,14,15] for a more detailed description of the method.

A further characterisation of the cascade debris was provided by the pair distribution function which, in its integral form, may be written as

$$G(r) = \frac{1}{N(N-1)} \sum_{i=1}^{N} \sum_{j>i}^{N} \delta(r - r_{ij}) \quad \text{where} \quad G(r) = \frac{4\pi r^2}{\Omega} g(r) \tag{1}$$

$g(r)$ being the standard pair correlation function where angular correlations are disregarded and Ω being the volume. In a structureless infinite homogeneous medium, $G(r)$ increases with r^2 while $g(r)$ is unity. $G(r)$ is normalized in such a way that

$$IG(R) = \int_0^R G(r)\mathrm{d}r \tag{2}$$

is unity when $R \geq r_{ij}^{\max}$, the largest separation distance between point defects in a cascade. The integral (2) will be used here to analyze pair separation distances between point defects in cascades over all distances within the simulation box.

The shortcoming of the BCA is that only the ballistic phase is properly modelled and further approximations are needed to allow for the effect of the thermal spike and the relaxation phase on the final defect distribution. The great advantage, however, is that it is several orders of magnitude faster than full MD and allows a much more statistically significant sampling of cascade debris to be accumulated, within limited computer time. Series of 500 cascades for each PKA energy, in the range from 5 to 100 keV, could thus be produced using the code Marlowe [16]. A PKA is introduced by providing a randomly chosen atom, located at a lattice site, with a momentum in a direction also selected at random, corresponding to a preset, well-defined initial kinetic energy. The ballistic phase of the cascade is then traced as a time ordered sequence of binary collisions of a moving projectile atom with a target atom assumed at rest, interacting by means of a repulsive pair potential used to compute the scattering integrals. We chose for this the so-called universal potential [17], also popular in full MD codes for modelling the interaction between 'close' encounters. The annealing phase of the cascade is then modelled by assuming a recombination radius between created SIA and neighbouring vacancies. This recombination radius was adjusted so as to predict the same number of Frenkel pairs (FP) as full MD [4]. The validity and limits of this method are extensively discussed in the literature [4,8–10,18–24].

Each series of cascades was then used as input to model the microstructure evolution, whose dependence on PKA energy could thereby be evaluated. The microstructure evolution has been simulated using the LAKIMOCA code. The method and the code are described in detail elsewhere [7]. The OKMC is compared to the rate equation approach in [25]. Briefly, in the OKMC, defects and defect clusters are treated as objects with specific positions in a simulation volume. The probabilities for thermally activated transition mechanisms are calculated based on Arrhenius frequencies. After a certain event is chosen to occur, time is increased according to a residence time algorithm [26]. The basic aspects of the parameterization used are described in [7]. Three parameter sets were used, which only differ by the SIAs and SIA clusters mobility models. In set I, all SIA clusters (size $m \geqslant 2$) migrate in 1D, with a migration energy $E_m = 0.04$ eV and a prefactor decreasing with the size m according to the law $\nu_0 m^{-s}$ ($\nu_0 = 6 \times 10^{12}\ \mathrm{s}^{-1}$, $s = 0.51$, following Ref. [27]). In set II, small clusters ($m \leqslant 5$) migrate in 3D with $E_m = 0.4$ eV, as broadly suggested by recent *ab initio* calculations [28], while larger clusters maintain 1D motion with $E_m = 0.04$ eV. For large clusters the prefactor decreases with $s = 0.51$ and for small ones it decreases with $s = 10$. Finally, set III treats small clusters ($m \leqslant 5$) in the same way as set II, but assumes that larger clusters are completely immobile (see Table 1). For

Table 1
Summary of parameter sets describing the SIA cluster mobility

SIA cluster size	Set I			Set II			Set III		
(E_m in eV)	s	E_m	D	s	E_m	D	s	E_m	D
$m = 1$	–	0.3	3D	–	0.3	3D	–	0.3	3D
$2 \leqslant m \leqslant 5$	0.51	0.04	1D	10	0.4	3D	10	0.4	3D
$m > 5$	0.51	0.04	1D	0.51	0.04	1D	Immobile		

More detail is given in Ref. [7].

vacancy clusters, the same mobility was used for all three sets: a migration energy of 0.65 eV and a prefactor decreasing with size according to the law $\nu_0 p^{-(m-2)}$ for $m \geqslant 2$, with $p = 100$ and again $\nu_0 = 6 \times 10^{12}\ s^{-1}$. These sets are summarized in Table 1. Cluster growth can take place by agglomeration of point defects of the same type, while defects of opposite type annihilate. These reactions are assumed to take place spontaneously whenever the two reacting defects happen to be at a mutual distance shorter than a predefined reaction radius. Spherical reaction volumes are implicitly assumed. The irradiation temperature was 343 K. With all sets, 100 ppm traps for SIAs and SIA clusters were included. These traps account for the role of impurity atoms on the SIAs mobility.

In each OKMC run, cascade debris were selected at random from the corresponding series of 500 samples and introduced in the simulation box according to a pre-assigned dose-rate (in dpa/s), until a pre-assigned dose (in dpa) was reached. The number of dpa (displacements per atom) was computed based on the NRT approximation [29]. Simulations for all PKA energies were performed at a dose-rate of 10^{-6} dpa/s, up to a dose of 0.1 dpa. These conditions are similar to those typical of materials test reactors. For a study of the sensitivity of the results to all parameters, dose-rates from 10^{-8} to 10^{-5} dpa/s and doses from 0.01 to 0.4 dpa have also been studied for a fixed PKA energy.

3. Independence of displacement cascades at given damage rate and dose

BCA cascades generated with the MARLOWE code served as input for the OKMC simulations with the LAKIMOCA code. As mentioned, the considered PKA energies ranged from 5 keV to 100 keV and the OKMC simulations were repeated for series of 500 cascades, each series corresponding to one PKA energy. In each OKMC run, cascades generated with a given PKA energy were selected at random according to a pre-assigned NRT damage

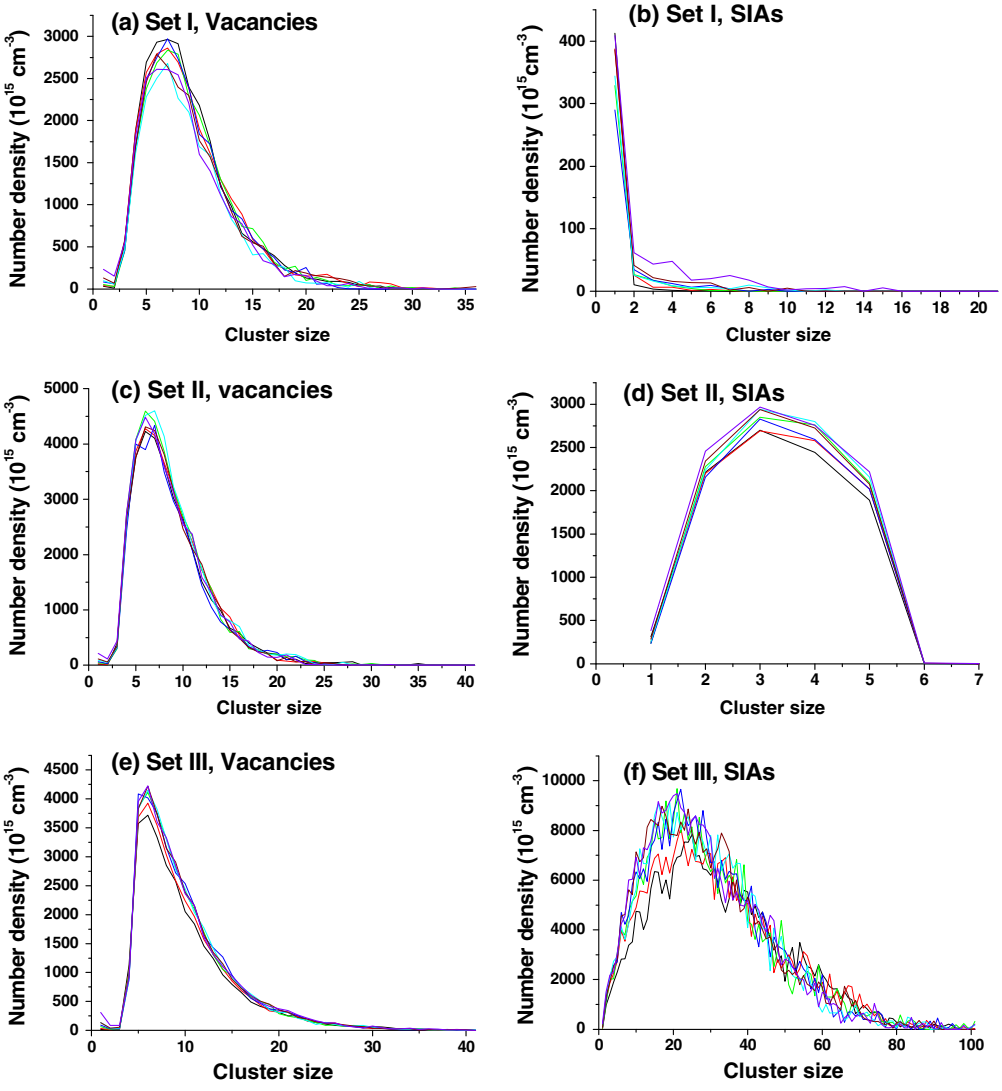

Fig. 1. Size distributions of vacancies (first column) and interstitial (second column) obtained with a dose-rate of 10^{-6} dpa/s and an irradiation dose of 0.1 dpa. Results in row 1 are obtained with the mobility parameters set 1, in row 2 with set 2 and in row 3 with set 3. PKA energies are 5, 10, 20, 30, 40, 50 and 100 keV.

rate, until a pre-assigned dose was reached. The damage rate was 10^{-6} dpa/s and the total dose 0.1 dpa. These conditions are relevant to high flux fission reactor working conditions. For each run, the growth of SIA and of vacancy clusters is followed by estimating their number densities and size distributions. Statistics has been accumulated over distributions in the last 0.01 dpa evolution. The calculations were repeated with each set of mobility parameters described in the previous section. The fractions of clustered vacancies and SIAs obtained with each series of input cascades are shown in Fig. 1 as functions of cluster size. For convenience, in what follows, such distributions will be termed 'clustered size distributions'. Although not coincident, 'clustered' size distributions bear the same information as 'cluster' size distributions and the distinction is thus not of prime importance. It can be seen that the obtained size distributions are independent of the PKA energy, although different OKMC mobility parameter sets produce completely different SIA clustered size distributions (the densities differ by a factor 20 from set 1 to set 3). Although the mobility of vacancies is the same for the three sets, their total number is sensitive to the model used for the mobility of small SIA clusters, due to recombination. This may be appreciated by comparing the vacancy clustered size distributions as obtained with sets 1 and 2.

The independence of clustered size distributions on the long term on the PKA energy suggests that not all cascade features are significant in cluster growth. They are now considered one after the other in this respect.

3.1. Subcascades

The partition of displacement cascades into subcascades was analysed by means of the fuzzy pattern recognition technique quoted in the previous section and the results are shown in Fig. 2.

The long term evolution of vacancy and SIA clusters growth is distinguished in the OKMC simulations; for this reason, the partitioning into subcascades was done separately for SIAs and vacancies, the objective being to characterise the initial distribution of clusters of one and the other type. Of course, these subcascades, defined on one defect population only and defined on the basis of defect positions, are merely 'geometrical' entities, rather than subcascades of collisions, triggered by secondary knock-on atoms, within which a priori the number of SIAs matches the number of vacancies. The mean number of these subcascades is a monotonically increasing function of the PKA energy, as shown in Fig. 2. The numbers are somewhat larger than those obtained by visualization techniques, because the algorithm allows overlapping subcascades to be detected, which is usually not considered when

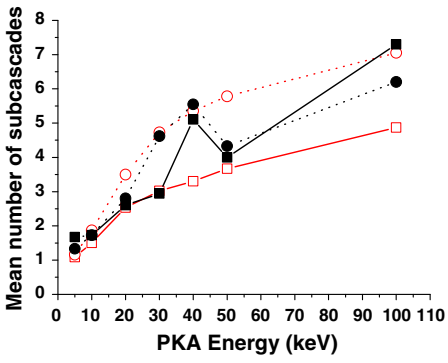

Fig. 2. Mean number of vacancy and of interstitial subcascades as a function of the PKA energy. Circles: vacancies, squares: SIAs; open symbols: BCA cascades, filled symbols: MD cascades.

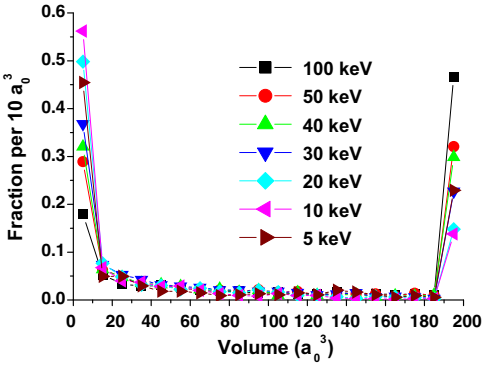

Fig. 3. Size distribution of subcascades as obtained with different PKA energies. a_0 is the lattice distance in iron.

using visualization. Results obtained from full molecular dynamics cascades are shown for comparison and are in good agreement with the BCA results.

Since the number of subcascades depends on the PKA energy, while the clustered size distributions on the long term do not, we conclude that subcascade formation is of no effect on the kinetics of cluster growth.

3.2. Subcascades extension

Fig. 3 shows distributions of subcascade volumes determined for the different considered PKA energies. Only SIA subcascades are shown, as the same trends are found for vacancy subcascades. These distributions are very widespread (the largest volumes are all cumulated in the last channel of the distributions). Here too, a dependence on the cascade energy is found. Except the case of

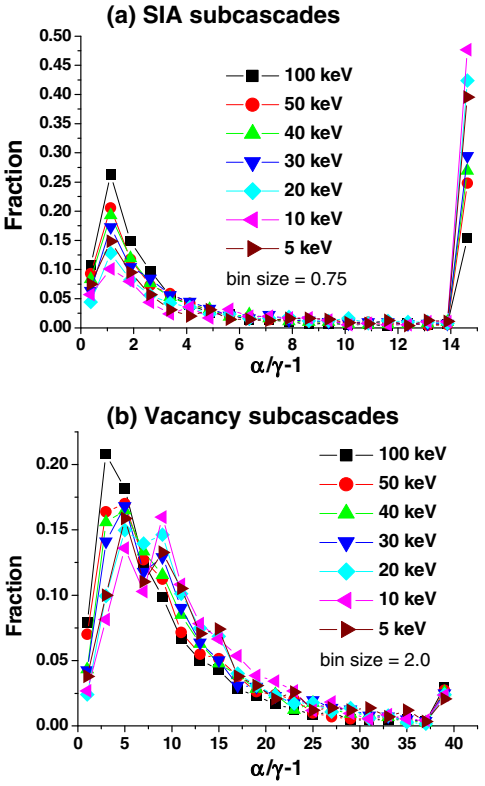

Fig. 4. Distributions of aspect ratios of subcascades obtained with different PKA energies.

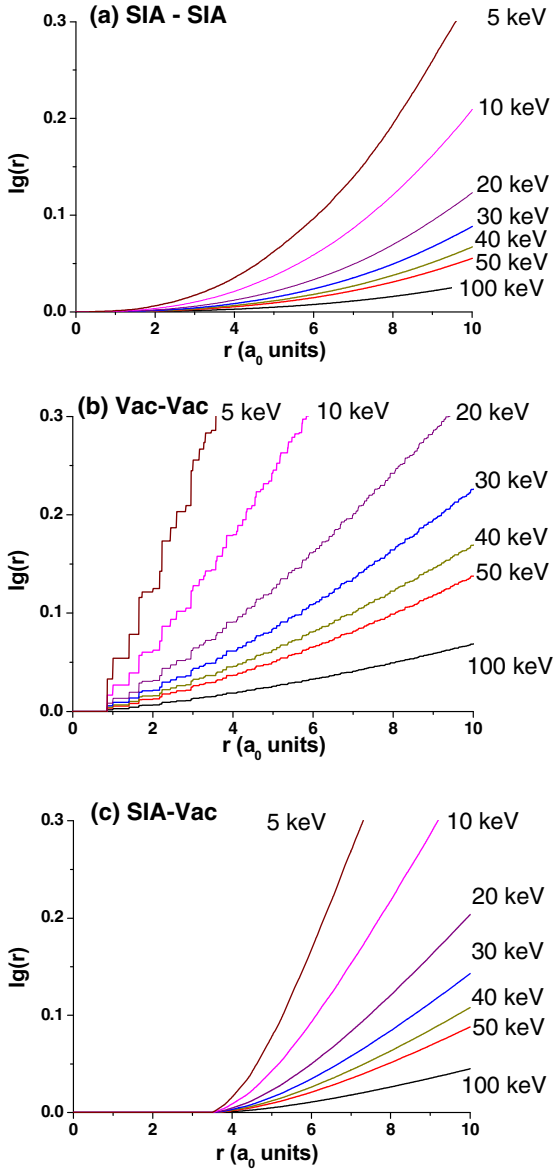

Fig. 5. Integrated pair distribution functions. Distributions are shown as obtained with different PKA energies (a) for SIA–SIA pairs, (b) for vacancy–vacancy pairs and (c) for vacancy–SIA pairs.

5 keV cascades, the number of small subcascades (first bin in the distributions of Fig. 3) decreases with increasing PKA energy while the opposite dependence is found for the largest ones (last bin in Fig. 3). Using the same argument as for the number of subcascades, we conclude that their spatial extension has no effect on the kinetics of the cluster growth either.

3.3. Subcascades morphologies

Aspect ratio distributions of the formed subcascades are shown in Fig. 4. As seen in the figure, all distributions display a mode for the same elongation. The distributions however display long tails (the most elongated subcascades are cumulated in the last channel). It is seen that the most elongated subcascades correspond to the lowest PKA energy while the frequency in the low elongation mode is an increasing function of the energy. Hence, the aspect ratio distributions are dependent on the PKA energy and, still using the same argument, one concludes that the kinetics of cluster growth is not sensitive to the initial morphology of subcascades.

3.4. Point defect spatial correlations

Integrated SIA–SIA, vacancy–vacancy and vacancy–SIA pair correlation functions Eq. (2) are shown in Fig. 5 for small separation distances. The slope at the origin is clearly a decreasing function

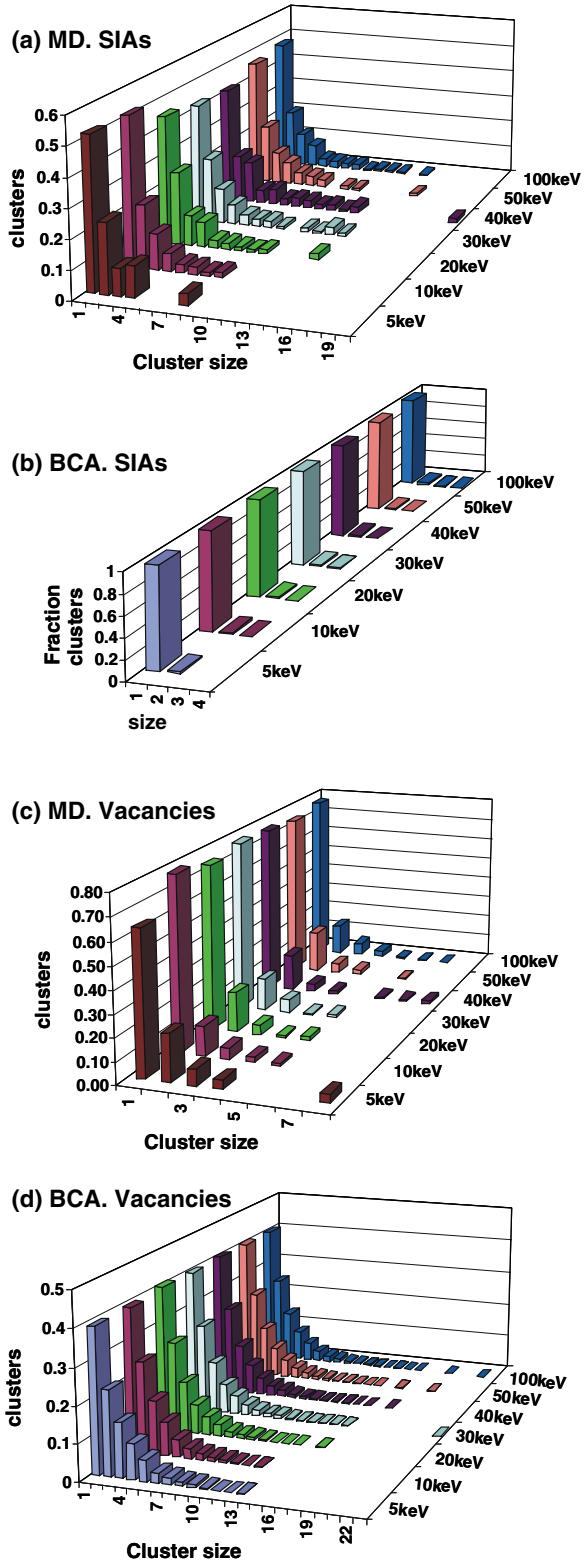

Fig. 6. Fractions of SIAs (a and b) and of vacancies (c and d) as functions of cluster size obtained at the end of displacement cascades generated with different PKA energies, as estimated by MD and by the BCA.

of the PKA energy, demonstrating that the separation between point defects is an increasing function of the PKA energy. Hence, the kinetics of cluster growth does not depend on point defect separation distances in cascades, either.

3.5. SIA and vacancy clusters

SIA and vacancy clusters have been detected on the basis of a second nearest neighbour criterion. Fig. 6 shows the fractions of SIAs and vacancies as functions of the clustered size, as obtained at the end of displacement cascades generated with different PKA energies. It is known that the BCA underestimates the efficiency of SIA clustering during the annealing phase of collision cascades [4,9]. Therefore, the clustered size distributions in MD cascades are shown too. In contrast with all the results presented in the previous sections, point defect clustered size distributions are found, within statistical error, to be independent of the PKA energy in the range investigated. Hence, these distributions, peaked at single-SIA and single-vacancies, and rapidly decreasing with clustered size, represent a cascade invariant and are the only cascade characteristics found, up to now, to be independent of the PKA energy. They may therefore have a role in determining the kinetics of their growth in the long term.

4. Dependencies on dose and dose-rate

Independently of the models used for predicting the long term growth of point defect clusters, dose and dose-rates are expected to be important factors in the growth kinetics. However, given the competition between the several possible reactions involved in the OKMC, no intuitive guideline allows even qualitative predictions on clustered size populations. For these reasons, the simulations presented in Section III were repeated for different dose-rates at constant dose and different doses at constant dose-rate. All results were found to be independent of the PKA energy.

4.1. The effect of dose-rate at 0.1 dpa irradiation dose

The results obtained with different dose-rates are given in Fig. 7. The dependence of the clustered size distribution on the

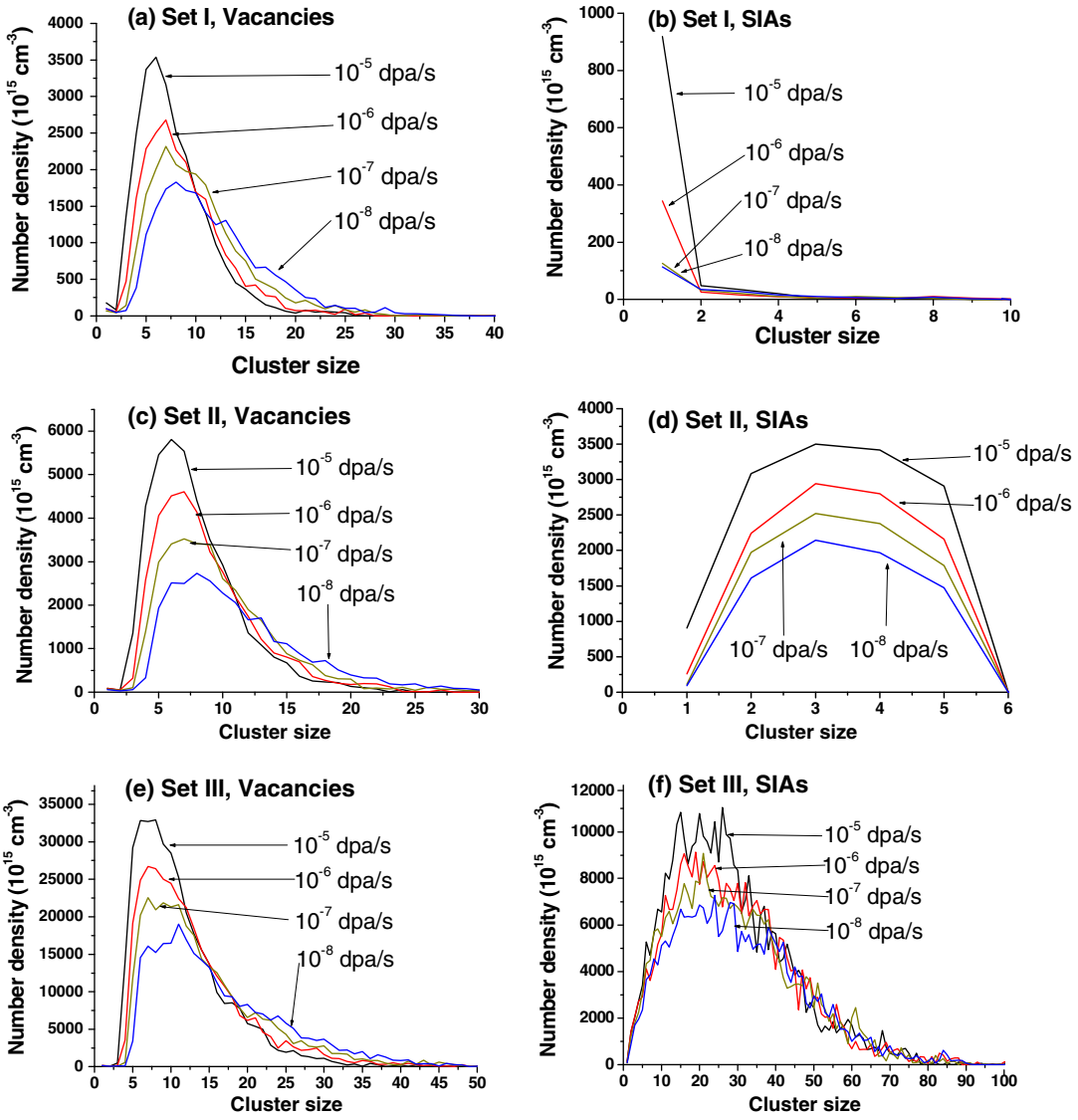

Fig. 7. Size distributions of number densities of vacancies in clusters (first column) and interstitials in clusters (second column) for the three sets of SIA mobility parameters used in the OKMC simulations. The PKA energy is 40 keV. Row 1: set 1, row 2: set 2, row 3: set 3. The results are presented as obtained for dose-rates from 10^{-8} dpa/s to 10^{-5} dpa/s.

dose-rate is obvious. It is not surprising that SIA clustered size distributions depend on the model used for describing their mobility. The consequences of considering the motion of small SIA clusters as 1D (set 1) or 3D (set 2) as well as considering the large SIA clusters as mobile or not (set 3) are dramatic. The model for describing the mobility of vacancy clusters is the same in each set. The clustered size distribution profiles are not much affected by the parameters governing the mobility of SIA clusters. However, quantitatively, the vacancy cluster densities differ by one order of magnitude between sets 1 and 3. The general trend when increasing the dose-rate is to enhance the population of small vacancy clusters and to decrease the population of large ones.

4.2. The effect of dose at a dose-rate of 10^{-6} dpa/s

Here again, as depicted in Fig. 8, the dependence of the distributions of dose is obvious. When large SIA are mobile and small SIA move 1D, only individual SIAs remain in the box, all clusters being absorbed by sinks or grain boundaries. The trapping at grain boundaries is more unlikely in the case of 3D SIA small clusters motion and a rather flat SIA clustered size distribution is obtained, limited at the size above which the evolution is governed by the mobility parameters for large clusters. Finally, if the large clusters are considered as immobile (set 3), they grow efficiently at the expense of smaller clusters. Except when large SIA clusters are immobile, vacancy clustered size distributions are very similar (their full width at half maximum does not differ by more than about 2 vacancies) although the tail is increasingly pronounced with higher doses. The vacancy clustered size distributions are significantly affected by the mobility parameters of large SIA clusters, the largest vacancy clusters being found when the largest SIA clusters are found too.

5. Discussion

Three aspects of the evolution of damage, with different characteristic times, have been considered in the previous sections. One aspect is the development displacement cascades which characteristic time is of the order of pico- to nano-second at the most. The second one is the dose-rate where the characteristic time involved

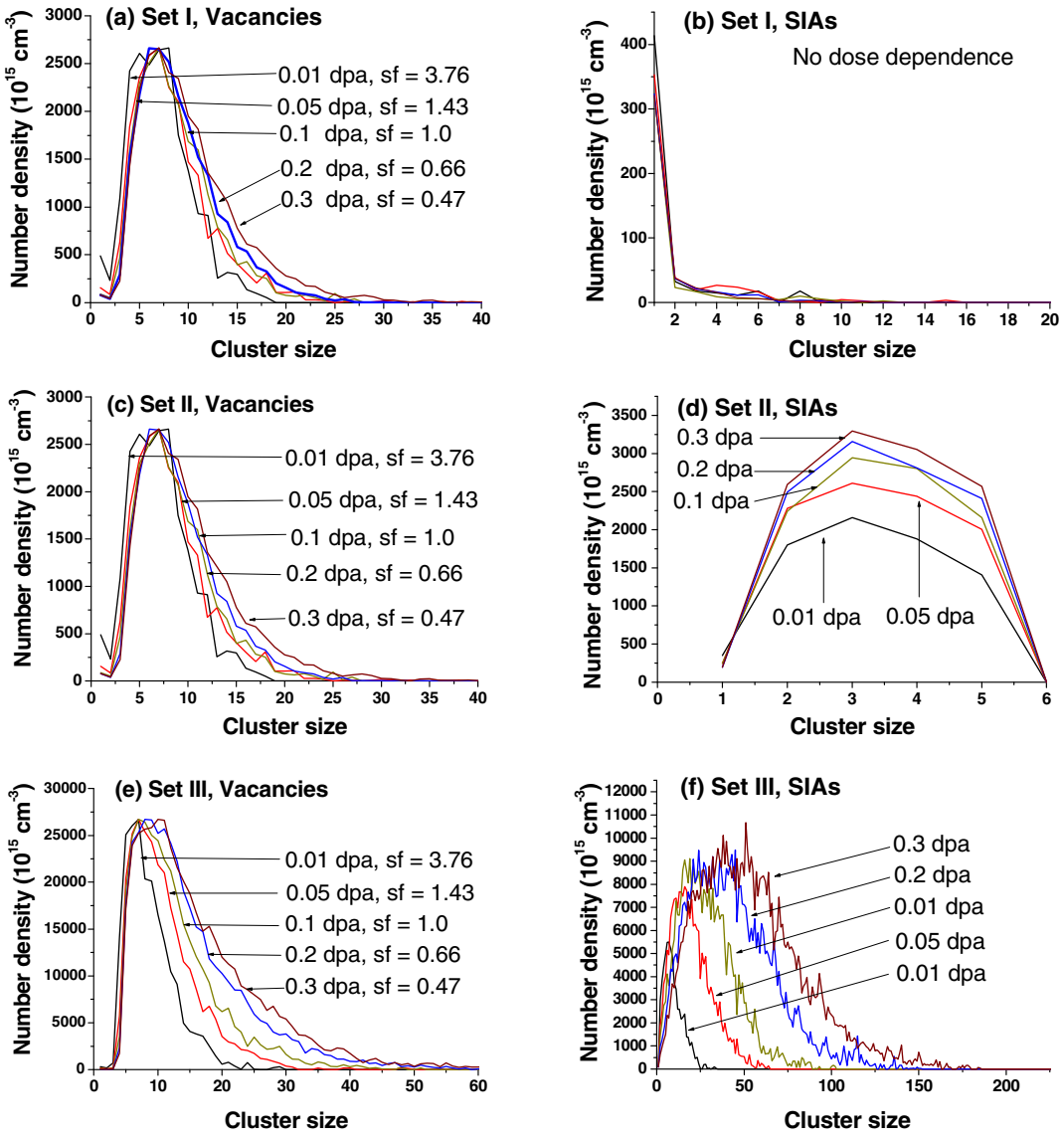

Fig. 8. Same as Fig. 7, but as functions of dose, for a dose-rate of 10^{-6} dpa/s. The mode of the size distributions for vacancies are normalized to the mode for a dose of 0.1 dpa, in order to visualize a comparison of distribution profiles. The scaling factors (sf) are given in the insets.

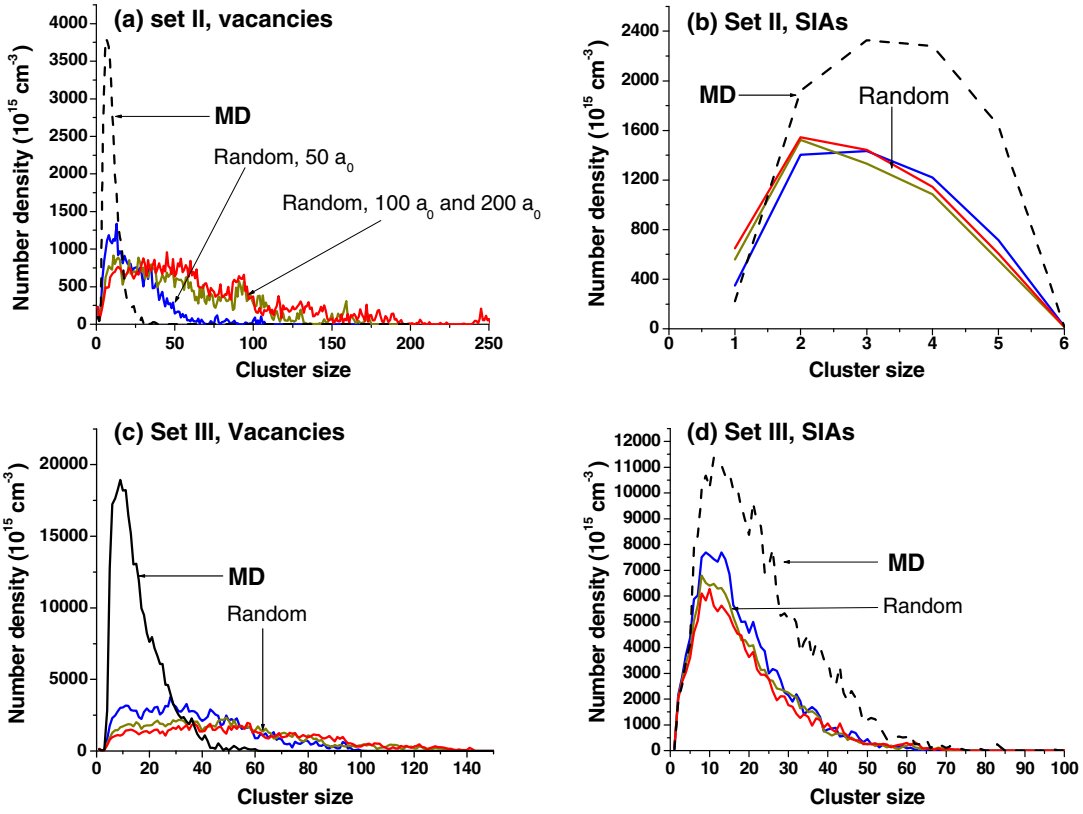

Fig. 9. Number densities of SIAs and of vacancy in clusters as functions of cluster size as obtained when selecting the initial location of pre-existing point defect clusters at random in the 64th, the 8th and the whole OKMC simulation box, using cluster size distributions in MD cascades. The results are compared with those obtained by injecting the MD cascades themselves. The dose is 0.1 dpa, the dose-rate is 10^{-6} dpa/s. When results are distinguishable, the sizes of the random selection areas are given in lattice units, a_0. The box is a cube of 200 a_0 size.

is the time interval separating the injection of an additional cascade in the OKMC simulation box, ranging between 3 and 60 s. The third one is the time to get the total dose, ranging from 10^4 to 10^7 s. Since these time scales are very different, the related phenomena may be expected to couple only weakly. It is indeed found that the long term evolution is not sensitive to the PKA energy and thus to the related cascade characteristics. In the previous section however, dose and dose-rate were found interrelated and it was suggested that a coupling may exist as cluster growth is governed by interrelated reactions and cluster diffusion times spanning over both time scales. These clusters find their origin in cascades and, as shown in Fig. 6, their size distribution does not depend on the PKA energy between 5 and 100 keV which memory is lost during the long term evolution. Consequently, the memory of their characteristics could be kept in the long term. The question thus arises whether these distributions represent the only cascade feature which may influence the long term evolution. A positive answer to this question would mean that the knowledge of the clustered size distribution would be the only needed information from cascades to correctly predict cluster evolution in the long term. This would represent a strong reduction of the number of parameters and a limited effort compared to building huge realistic cascades data banks. Part of the answer was already given in [10], where it was shown that spatial correlations between point defects in displacement cascades do matter in the long term evolution. Here, we raise the question of the spatial distribution of the initial point defect clusters. The main feature of cascades is indeed the spatial confinement of the produced point defect clusters. In order to know if this confinement matters on the long term, additional OKMC simulations were performed, using the same dose-rate of 10^{-6} dpa/s and dose of 0.1 dpa, but selecting the initial locations of the pre-existing point defect clusters at random and in limited zones of the OKMC box, namely, the 64th, the 8th of it, as well as the whole simulation box. The clustered size distributions used were those published in [10]. The results obtained with sets 2 and 3 are shown in Fig. 9.

Using the clustered size distributions in [10] and shown in Fig. 6 for MD cascade, a dose of 0.1 dpa with 10^{-6} dpa/s dose-rate could not be reached within affordable CPU time with set 1, which already demonstrates a major difference in growth kinetics.

The results of Fig. 9 indicate that selecting primary vacancy and interstitial clusters at random in zones of different sizes in the simulation box does not have big consequences on the clustered distributions on the long term. Hence, the results appear not to be sensitive to the mean number densities of point defect clusters, insofar as the confinement effect is not even stronger than considered here. However, these new distributions are significantly at variance with the clustered size distributions obtained on the long term using SIA and vacancy clusters distributions from MD cascades. The divergence is particularly striking in the case of vacancy clusters, where the number densities obtained with the MD cascades are a factor 5–10 larger then when using the same clusters distributed at random in the box. This shows that not only the clustered size distributions, but also the spatial correlations between clusters affect the cluster populations in the long term.

6. Conclusion

We have shown that the evolution of vacancy and SIA clustered size distributions in the long term only depend on a limited number of characteristics of the primary damage, as represented by BCA cascades in a 5–100 keV of energy. In particular, we showed

that clustered size distributions in the long term do not significantly depend on the PKA energy in the considered range. Hence, the PKA recoil spectrum is probably not a critical parameter to be allowed for in the long term damage evolution. Several cascade characteristics, namely, the splitting of cascades into subcascades, the spatial extent and the aspect ratio of subcascades, as well as spatial correlations between point defect positions, were found to depend on the PKA energy in the 5–100 keV range. Since the PKA energy does not affect the long term evolution, these characteristics do not either. Conversely, point defect clusters resulting from displacement cascades represent a cascade invariant, in the sense that they do not depend on the recoil energy and the spatial correlations characterising these initial clustered defect distributions do influence the long term cluster growth. This suggests that mean field approximations in which the source terms are transformed into spatially uniform distributions of clusters will be applicable only to a limited number of cases. On the other hand, whether point defect clustered distributions and their spatial correlations are the only cascade parameters determining cluster growth in the long term, or other parameters of importance exist, is a question yet to be answered. For sure, as expected and demonstrated in the present work, not only dose, but also dose-rate have a major influence on long term cluster growth.

Acknowledgements

This work was prepared in the framework of the integrated project PERFECT (F160-CT-2003-508840) under program EURATOM FP-6 of the European Commission.

References

[1] J.B. Gibson, A.N. Goland, M. Milgram, G.H. Vineyard, Phys. Rev. 120 (1960) 1229.
[2] M.T. Robinson, I.M. Torrens, Phys. Rev. B 9 (1974) 5008.
[3] M. Hou, A. Souidi, C.S. Beckaert, J. Phys. C 13 (2001) 5365.
[4] A. Souidi, M. Hou, C.S. Becquart, C. Domain, J. Nucl. Mater. 295 (2001) 179.
[5] <https://www.fp6perfect.net/site/index.htm>.
[6] C.S. Becquart, C. Domain, A. Legris, J-C. Van Duysen, J. Nucl. Mater. 280 (2000) 73.
[7] C. Domain, C.S. Becquart, L. Malerba, J. Nucl. Mater. 335 (2004) 121.
[8] C.S. Becquart, C. Domain, L. Malerba, M. Hou, Nucl. Instrum. and Meth. B 228 (2005) 181.
[9] C.S. Becquart, A. Souidi, C. Domain, M. Hou, L. Malerba, R.E. Stoller, J. Nucl. Mater. 351 (2006) 39.
[10] A. Souidi, C.S. Becquart, C. Domain, D. Terentyev, L. Malerba, A.F. Calder, D.J. Bacon, R.E. Stoller, Yu.N. Osetsky, M. Hou, J. Nucl. Mater. 355 (2006) 89.
[11] R.E. Stoller, J. Nucl. Mater. 233 (1996) 999;
R.E. Stoller, G.R. Odette, B.D. Wirth, J. Nucl. Mater. 251 (1997) 49;
R.E. Stoller, A.F. Calder, J. Nucl. Mater. 283 (2000) 746;
R.E. Stoller, Nucl. Eng. Design 195 (2000) 129;
R.E. Stoller, S.G. Guiriec, J. Nucl. Mater. 329 (2004) 1238.
[12] M.W. Finnis, MOLDY6-A Molecular Dynamics Program for Simulation of Pure Metals, AERE R-13182, UKAEA Harwell Laboratory, Harwell, UK, 1988.
[13] M.W. Finnis, J.E. Sinclair, Philos. Mag. A 50 (1984) 45;
M.W. Finnis, J.E. Sinclair, Erratum, Philos. Mag. A53 (1986) 161.
[14] M. Hou, Phys. Rev. B 31 (7) (1985) 4178.
[15] M. Hou, Phys. Rev. A 39 (6) (1989) 2817.
[16] M.T. Robinson, Phys. Rev. B 40 (1989) 10717.
[17] J.F. Ziegler, J.P. Biersack, U. Littmark, in: Stopping and Ranges of Ions in Solids, Pergamon, New York, 1985. 25.
[18] M. Hou, Z. Pan, Nucl. Instrum. and Meth. B 90 (1994) 468.
[19] M. Hou, Z. Pan, Nucl. Instrum. and Meth. B 102 (1995) 93.
[20] M. Hou, Z.Y. Pan, Rad. Eff. Defects Solids 142 (1997) 94.
[21] C.S. Becquart, M. Hou, A. Souidi, Mater. Res. Symp. Proc. 650 (2001) R4.3.1.
[22] M. Hou, A. Souidi, C.S. Becquart, Nucl. Instrum. and Meth. B 196 (2002) 31.
[23] C.S. Becquart, A. Souidi, M. Hou, Phys. Rev. B 66 (2002) 134104.
[24] C.S. Becquart, A. Souidi, M. Hou, Philos. Mag. A 4–7 (2005) 409.
[25] C. Ortiz, M.-J. Caturla, Phys. Rev. B 75 (2007) 184101.
[26] W.M. Young, E.W. Elcock, Proc. Phys. Soc. 89 (1966) 735.
[27] Yu.H. Osetsky, D.J. Bacon, A. Serra, B.N. Singh, S.I. Golubov, J. Nucl. Mater. 276 (2000) 65.
[28] F. Willaime, C.C. Fu, M.C. Marinica, J. Dalla Torre, Nucl. Instrum. and Meth. B 228 (2005) 92.
[29] M.J. Norgett, M.T. Robinson, I.M. Torrens, Nucl. Eng. Design 33 (1975) 50.